applied sciences

MDPI

Article

Effect of High Hydrostatic Pressure Processing on Starch Properties of Cassava Flour

Ladie Anne Conde [1,2], Biniam Kebede [1], Sze Ying Leong [1,3] and Indrawati Oey [1,3,*]

[1] Department of Food Science, University of Otago, Dunedin 9054, New Zealand
[2] Philippine Root Crop Research and Training Center (PhilRootcrops), Visayas State University, Baybay City 6521, Leyte, Philippines
[3] Riddet Institute, Palmerston North 4442, New Zealand
* Correspondence: indrawati.oey@otago.ac.nz; Tel.: +64-479-8735

Abstract: The aim of this study was to utilize high-pressure processing (HPP) to modify cassava flour through altering the starch components. Specifically, the effect of HPP processing variables, i.e., pressure (0.10 or untreated, 300, 400, 500, and 600 MPa), flour concentration (FC; 10, 20, and 30%), and holding time (HT; 10 and 30 min) on starch-related properties was studied. Microstructural integrity, thermal properties, and starch susceptibility to digestive enzymes were determined. A three-way ANOVA was performed to identify the interaction effect between these process variables. In general, 600 MPa consistently transformed the crystalline starch into an amorphous one. HPP-induced gelatinization led to enlarged starches with loss of birefringence, reduced relative crystallinity percentage, and changes in short-range order. The three-way interaction between the process variables was evident in the significant progressive rise in onset gelatinization temperature and degree of gelatinization, and the decline in gelatinization enthalpy from 500 to 600 MPa with decreasing FC and increasing HT. These changes caused an increased percentage of rapidly digestible starch and decreased resistant starch fraction. Overall, this study's results imply the possibility of using HPP to modify the starch component in cassava flour and potentially create flours with varying levels of functionalities.

Keywords: high pressure; cassava flour; starch; physical modification; digestibility

Citation: Conde, L.A.; Kebede, B.; Leong, S.Y.; Oey, I. Effect of High Hydrostatic Pressure Processing on Starch Properties of Cassava Flour. *Appl. Sci.* **2022**, *12*, 10043. https://doi.org/10.3390/app121910043

Academic Editor: Anabela Raymundo

Received: 9 September 2022
Accepted: 4 October 2022
Published: 6 October 2022

1. Introduction

Cassava (*Manihot esculenta* Crantz) is a root crop harvested for its starchy underground tuber and is second to maize as a staple starch source [1]. Therefore, it is a highly valued agricultural crop in developing countries. Cassava flour is made from the whole edible portion of its roots and is mainly utilized in baked products and sometimes alcohol production [2,3]. The flour is typically composed of approximately 67–88% starch and 1–5% fiber, and a much smaller amount of protein, fat, and ash [4,5]; its functionality is majorly driven by its starch.

High hydrostatic pressure (HHP) modification of food biopolymers, specifically starches, offers a non-thermal approach to gelatinization and physical modification [6]. Several studies have looked at the effect of HPP processing parameters on isolated starches from various botanical origins, crystallinity patterns, and amylose content. Differences in the degree of gelatinization, crystallinity, and pasting properties were found to depend on the type of starch and the HPP processing parameters, i.e., pressure–temperature combination, holding time, starch concentration, and suspending media [6–9]. In general, HPP-modified starch (in water suspensions) is gelatinization-driven and is characterized by (1) imposed permeation of water into crystalline and amorphous regions of granules that lead to irreversible swelling and gelatinization of starch granules, (2) partial or complete gelatinization of the starch granule's internal regions below the gelatinization onset

temperatures induced by heat treatment, and (3) the granular shape staying intact even after HPP [6].

However, fewer studies have been dedicated to starchy matrices such flour. To date, flours subjected to HPP were mainly of cereal, pseudo cereal, grain, and legume origin [10–13]. Most of the studies looked at noodle, batter, dough, and bread quality of single or composite flours subjected to HPP [14–16]. Like isolated starches, the effect of increasing pressure on the flour's gelatinization temperatures varied depending on botanical origin, hydration level, and pressurizing time, but consistently decreased the enthalpy of gelatinization. Previous studies have also observed a reduction of pasting properties for HHP-treated flours due to the pressure-induced starch gelatinization that disrupts the crystalline structure [10,13,14,16,17], which consequently lowers its retrogradation tendency [18].

The objective of this study was to utilize HPP to modify cassava flour as a function of HPP processing parameters (i.e., pressure level and pressure holding time) and flour concentration. Since cassava is a poor source of protein and fat, the current study focused only on starch modification through HPP. Three-way ANOVA was applied to identify possible interaction effects between process variables. This allows for a wide-ranging study on the impact of HPP processing variables on cassava flour and informs the food industry of potential new applications.

2. Materials and Methods

2.1. Cassava Flour and Slurry Preparation

Philippine cassava cultivar NSIC Cv-13 was provided by PhilRootcrops of Visayas State University, Leyte, Philippines. The flour had 12.24% moisture, 3.12% ash, and 81.04% starch. Cassava flour slurry was prepared by mixing 10 g of flour and distilled water in a 10, 20, and 30% (w_{db}/v) flour concentration (FC) in clear vacuum pouches. Samples were made in triplicates, sealed with as much air removed as possible, and kept chilled until processing.

2.2. HHP Processing of Cassava Flour

HHP processing was carried out using Multivac HPP 055 (Multivac Sepp Haggenmüller GmbH and Co., Wolferschwenden, Germany) at different predefined pressure levels (300, 400, 500, and 600 MPa) combined at room temperature for 10 and 30 min holding time (HT). Water with an initial temperature of 5 ± 1 °C was used as a pressure-transmitting medium in a 55 L chamber, and its final temperature did not exceed 31 °C. Pressure build-up was conducted at 100 MPa/min with a similar decompression rate after the targeted holding time was achieved. All treated and untreated (0.1 MPa) samples were freeze-dried and stored in laminated foil pouches at 4 °C until further analysis. The samples were coded based on pressure level–flour concentration–holding time, e.g., 300–10%–10 means that the sample (10% flour concentration) was treated at 300 MPa for 10 min. After treatment, a visual examination of slurry samples was carried out and photos were taken using a Canon EOS 6D Mark II camera (Oita City, Tokyo, Japan).

2.3. Morphological and Microstructural Analyses

2.3.1. Light and Polarized Microscopy

Fresh control and treated flour slurries were diluted to 0.05% (w/v) with ultrapure water, transferred to glass slides, and viewed under an Olympus BX41-P microscope (Olympus, Tokyo, Japan) at 400× magnification. The observations were captured through an attached Canon EOS 1100D camera (Oita City, Tokyo, Japan). Native starch is birefringent, displaying a Maltese cross under polarized light owing to its radially oriented crystalline structure [19]. Polarized images were also captured through the U-AN360P attachment (Olympus, Tokyo, Japan).

2.3.2. FTIR-ATR Analysis

The short-range ordered starch structure in cassava flour samples was determined from acquired spectra using a Bruker Optics FTIR Spectrometer (Alpha System, Framingham, MA, USA) with the ATR platinum diamond one accessory. Cleaning of the ATR crystal with isopropanol-soaked delicate wipes and background scanning were done prior to each sample scan. The spectrum was scanned from 400 to 4000 cm^{-1} with 32 scanning times at 4 cm^{-1} resolution. Baselines of generated spectra were corrected using OPUS software (Version 8.1, Bruker Optik, Ettlingen, Germany). These spectra were deconvoluted based on the second-order derivative peak identification [20] using OMNIC software (Thermo Scientific Fisher Inc., Waltham, MA, USA). Fitting was targeted at the 1200–875 cm^{-1} region, which is associated with the short-range order of starch. The ratio of the peak height of the absorbances around 1047 and 1022 cm^{-1} (Abs 1047/1022) was used to quantify the ordered and amorphous structure of the flour's starch [21–23], while the ratio of absorbance at 1022 and 995 cm^{-1} (Abs 1022/995) was used to measure the molecular order of starch double helices inside the crystallites [21,24].

2.3.3. X-ray Diffraction (XRD) Analysis

The long-range crystalline order of starch in cassava flour samples was determined using an X'Pert Pro MPD PW 3040/60 X-ray diffractometer (Malvern PANalytical, Almelo, Netherlands) operated at 40 kV and 30 mA with 2θ Cu Kα (λ = 1.5406 Å) irradiation in the diffraction angle range of 5–35°. The generated graph was processed using HighScore software v4.0 (Malvern PANalytical). Using the Origin Pro 2018 software (OriginLab Corporation, Northampton, MA, USA), the area under prominent peaks and total area under the curve were determined to calculate relative crystallinity (%RC) [25].

2.4. Determination of Thermal Properties Using Differential Scanning Calorimeter

Transitional thermal properties were determined using a TA Instruments Q2000 differential scanning calorimeter (New Castle, DE, USA). Hermetically sealed in an aluminum pan were approximately 5 mg of flour dispersed with distilled water (1:3 *w*/*v*). The pans were equilibrated for a minimum of 2 h at room temperature prior to analysis. These were then heated from 25–130 °C at a 5 °C/min rate with an empty sealed pan as a reference and a nitrogen flow of 50 mL/min. Analysis was carried out in triplicates, and the equipment's enthalpy and temperature were calibrated using indium. The generated peaks were integrated using TA Instruments Universal Analysis 2000 Version 4.5A software (New Castle, PA, USA) to determine the following parameters: onset (*To*), peak (*Tp*), and conclusion (*Tc*) temperatures, as well as gelatinization enthalpy (ΔH). The temperature range of gelatinization (*Trange*) was calculated as $2 * (Tp - To)$ according to Krueger et al. [26]. The degree of gelatinization (*DG*) was calculated as the percentage ΔH relative to the untreated flour.

2.5. Determination of Starch Susceptibility to Human Simulated Digestive Enzymes

Susceptibility of starch in cassava flour samples to digestive enzymes was evaluated using a three-stage static in vitro digestion method according to Minekus, et al. [27] with modifications. Flour samples (0.5 g) were placed in a 100 mL Schott bottle and hydrated with a recorded amount of ultrapure water 1 h before analysis.

2.5.1. Preparation of Digestion Solutions

Solutions were prepared according to the work of Abduh et al. [28]. "Saliva juice" was prepared by mixing 0.117 g (22 mM) NaCl, 0.149 g (2 mM) KCL, and 2.1 g (25 mM) $NaHCO_3$ in 1 L ultrapure water. A 0.0125 g/mL α-amylase solution was prepared by mixing *Aspergillus oryzae* α-amylase (Sigma, 30 U/mg, St. Louis, MO, USA) with ultrapure water. The gastric solution was prepared by adding 8.8184 g (151 mM) NaCl and 2.1 g KCL (28 mM) to 1 mM HCl (pH 3). To 100 mL of gastric solution, 4 g porcine stomach pepsin (AppliChem A4289, 0.7 FIP-U/mg, Barcelona, Spain) was added to make the "gastric juice". The "intestinal juice" was prepared by adding 1 g of porcine pancreas pancreatin

(Sigma P1750, 4 × USP, St. Louis, MI, USA) and 0.8452 g of porcine bile extract (ChemCruz SC-214601, Dallas, TX, USA) into 100 mL of 0.1 M $NaHCO_3$ (pH 7). All solutions with enzymes are prepared on the day of the assay and kept chilled until use. Additionally, 1 M HCl and 1 M NaOH were also prepared.

2.5.2. In Vitro Digestion Procedure

For stage 1 or the oral phase, the hydrated flour samples were mixed with 8 mL saliva juice and incubated at 37 °C (Contherm Scientific Ltd., Hutt City, New Zealand) for 5 min on a shaker (DLAB, SK-R1807-S, Hong Kong) with rocking motion (55 strokes/min). Afterwards, 2 mL of α-amylase solution was added and incubated for another 5 min. Then, the pH of the solution was adjusted to 3 with 1 M HCl to deactivate amylase. In stage 2 or the gastric phase, the acidic mixture was added to 8 mL gastric juice and incubated for 120 min with rocking. Then, pH was adjusted to 7 with 1 M NaOH to deactivate pepsin. For stage 3 or the intestinal phase, 16 mL of intestinal juice was added into the neutralized digest and incubated with rocking. Aliquots of 0.5 mL were collected at 20 and 120 min, with immediate heat shocking in boiling water for 10 min for enzyme deactivation. All of the collected digests were added to 2.5 mL of 100 mM sodium acetate buffer (pH 5), vortexed, and stored at 4 °C until glucose analysis within 24 h.

2.5.3. Measurement of Hydrolyzed Starch

The diluted digests were centrifuged at 2056× g (Beckman GPR Centrifuge, Brea, CA, USA) for 20 min at 20 °C. Supernatant aliquots of 50 µL, which contain all of the glucose released during enzymatic hydrolysis, were transferred into microtubes. To this, 1.5 mL of GOPOD reagent (Megazyme, Wicklow, Ireland) was added and mixed, and microtubes were incubated in a water bath (Grant, Cambridge, UK) at 50 °C for 20 min. The absorbance of the mixture was measured using a microplate reader at 510 nm (BioTek® Synergy™ 2, Winooski, VT, USA) and the glucose produced was calculated against a 100 mM sodium acetate buffer (pH 5) blank and glucose standard (1 mg/mL in 0.2% benzoic acid, Megazyme). Susceptibility to digestive enzymes was assessed through the determination of the percentage of rapidly digestible starch (RDS), slowly digestible starch (SDS), and resistant starch (RS) produced. These were calculated according to Equations (1)–(3):

$$\text{RDS}\ (\%) = \frac{(G_{20} - FG) \times 0.9}{TS} \times 100 \quad (1)$$

$$\text{SDS}\ (\%) = \frac{(G_{120} - G_{20}) \times 0.9}{TS} \times 100 \quad (2)$$

$$\text{RS}\ (\%) = \frac{TS - (\text{RDS} + \text{SDS})}{TS} \times 100 \quad (3)$$

where G_{20} and G_{120} are the amount of glucose released during intestinal starch hydrolysis at 20 and 120 min, respectively; FG is the amount of inherent free glucose in the flour; 0.9 is an adjustment to convert glucose into anhydroglucose (as occurs in starch); and TS is the total starch content of the flour [29]. The initial free glucose and total starch content of flour samples were determined using the Megazyme K-TSTA kit.

2.6. Statistical Analysis

Results are presented as mean values ± standard deviation. Three-way ANOVA was performed to compare the means of studied parameters for flours subjected to different pressure levels, flour concentration, and holding time at a 5% significance level using SPSS version 28 (IBM Corp., Armonk, NY, USA). For dependent variables with significant three-way interaction, the succeeding simple two-way interaction, simple simple main effects, and simple simple comparisons were carried out in sequence with Bonferroni correction on the significance level. If only two-way interaction was significant, simple main effects and simple comparisons were run for the processing variables involved.

3. Results and Discussion

3.1. Visual Examination of Freshly Treated Cassava Flour

No visible differences in the flour slurries were observed between untreated samples (Figure 1A) and all treatment combinations from 300–500 MPa except for 500–10%–30, which exhibited a slight increase in slurry viscosity. The 600–10%–10 (Figure 1(B1)) revealed a biphasic sample with opaque clumps of hydrated flour engulfed in a slightly viscous slurry, whereas 600–20%–10 and 30%–10 (Figure 1(B2,B3)) had turned into one uniform opaque clump with a reduced slurry. Increasing the holding time to 30 min at 600 MPa led to clumps with increasing translucency, with 10% FC still biphasic but increased slurry viscosity, whereas 20% and 30% hardly had excess slurry (Figure 1(C1–C3), respectively). These changes imply water uptake of flour by HPP-induced gelatinization and can be further visually validated through a microscopic evaluation.

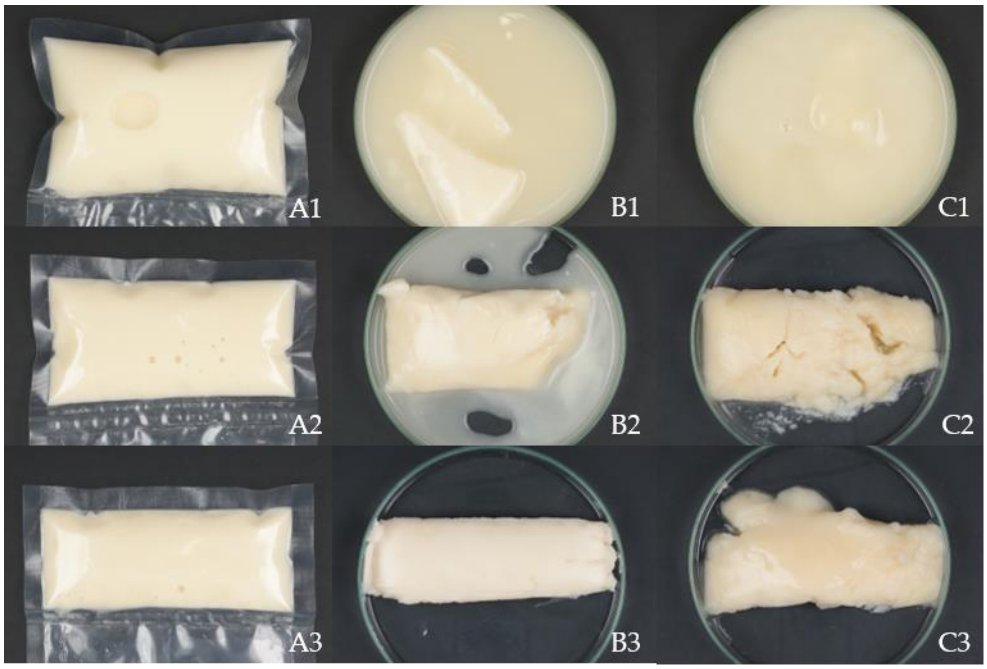

Figure 1. Visual changes of untreated and selected treated cassava flour slurries; where (**A1**) is 0.10 MPa, 10% flour concentration; (**A2**) is 0.10 MPa, 20% flour concentration; (**A3**) is 0.10 MPa, 30% flour concentration; (**B1**) is 600 MPa–10 min, 10% flour concentration; (**B2**) is 600 MPa–10 min, 20% flour concentration; (**B3**) is 600 MPa–10 min, 30% flour concentration; (**C1**) is 600 MPa–30 min, 10% flour concentration; (**C2**) is 600 MPa–30 min, 20% flour concentration; (**C3**) is 600 MPa–30 min, 30% flour concentration.

3.2. Birefringence of Cassava Starches in HPP-treated Cassava Flours

Microscope images showed varied sizes of cassava starch granules, as they have been reported to have a diameter ranging from 2.4–35 µm [30,31]. The cassava starch granule has a spherical morphology with a truncated side, similar to these untreated samples but with a few distorted and damaged granules probably sustained during flour processing. There was no visible difference between untreated cassava flours, 300–400 MPa combinations, and 500 MPa for 10 min holding time. The micrographs of 500–30 min and all 600 MPa combination treatments revealed enlarged and swelled starch granules as well as aggregation (Figure 2; solid yellow arrow), which explains the notable change in viscosity of the slurries and formation of gel-like clumps. Starch granule aggregation was also reported for cassava starch at 600 MPa [32], leading to gel formation [33–35]. Other flours also showed granule aggregation [11,36] and a more continuous protein distribution [37]. Despite the swelling of starch granules in the cassava flour, there was minimal granular disintegration, a characteristic of HPP-treated starches [6].

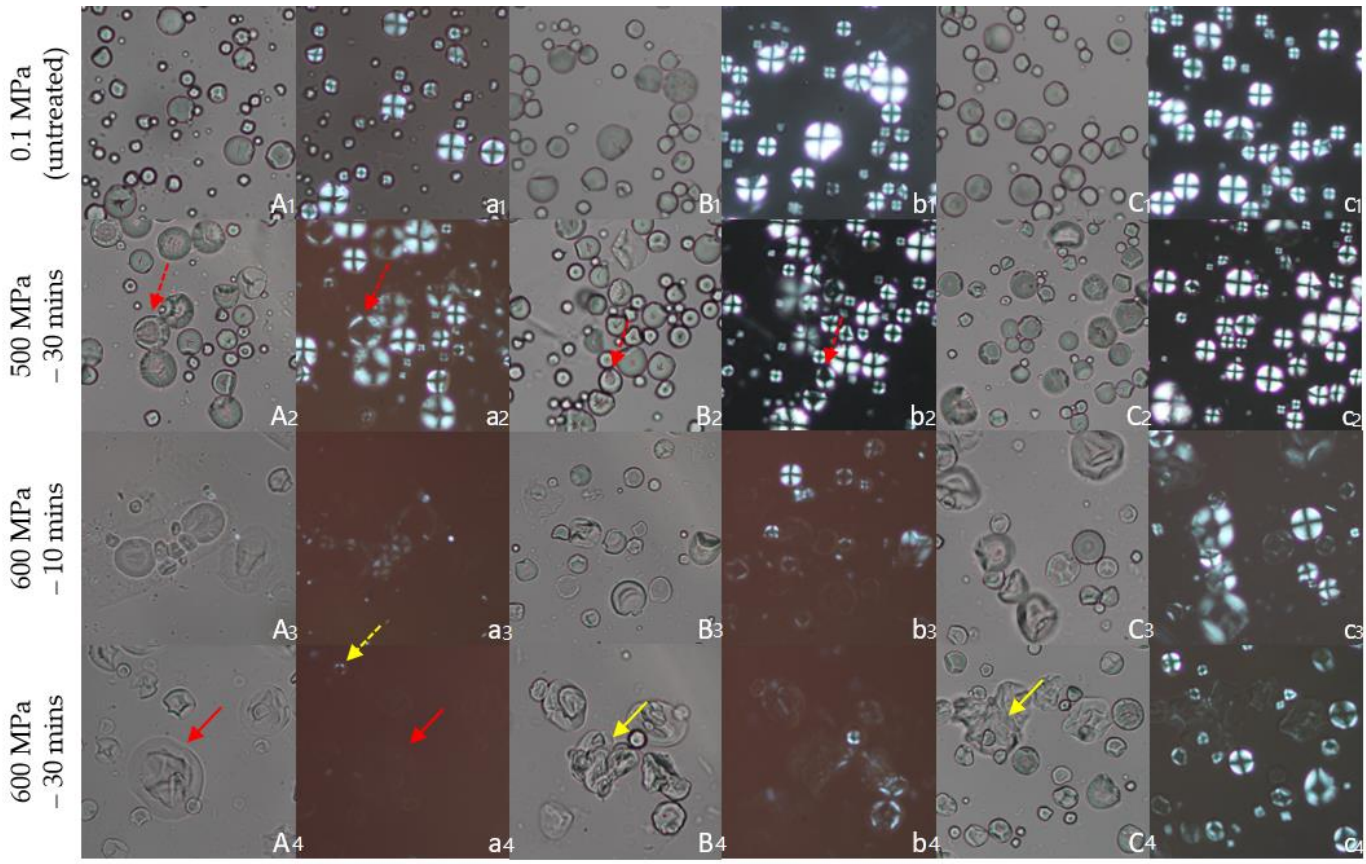

Figure 2. Light (**A1**–**A4**,**B1**–**B4**,**C1**–**C4**) and polarized (**a1**–**a4**,**b1**–**b4**,**c1**–**c4**) micrographs of untreated (0.10 MPa) and selected treated cassava flour suspensions at 400× magnification; where (**A1**–**A4**,**B1**–**B4**,**C1**–**C4**) represent 10%, 20%, and 30% flour concentration, respectively.

Polarized images of the flours revealed a Maltese cross pattern due to the radial orientation of the crystallites [19], as shown in Figure 2. Similar to light micrographs, untreated cassava flours, all 300–400 MPa combinations, and 500–10 min did not exhibit loss of birefringence (photos not shown). As seen from the starch granules' swelling, the 500–30 min and all 600 MPa combination treatments caused a visible dissolution of the Maltese cross. This phenomenon is intensified by increasing pressure levels, prolonging holding time, and decreasing flour concentration. This birefringence loss indicates the disorganization of molecular crystalline order [38] that came with pressure-induced gelatinization. At 500–30 min, the number of swollen starch granules increased with a decrease in flour concentration. Some swollen starch granules showed a hollow and gel-like center that appeared dark in polarized light with birefringence in the periphery (Figure 2; dashed red arrow). This suggests a loss of radial orientation and organization, supported by the report of Błaszczak et al. [39], wherein two distinct zones were seen from sliced HPP-treated potato starch granules, with the outer zone corresponding to unchanged structures and a gel-like network in the inner zone. Highly enlarged starch granules that showed no cross pattern (Figure 2; solid red arrow), indicating a complete loss of birefringence, were abundant in 600–10% FC samples, followed by 20% and least at 30% FC. All 600–30 min treatments had visually more loss of birefringence than their 600–10 min counterparts.

Complete loss of birefringence was reported for isolated cassava starch granules from 550 MPa at 30%–30 min [40] to 600 MPa at 20%–5 min [34] and 50%–30 min [32], indicating pressure–concentration–time dependence. A similar finding can be reported for cassava flour, with a gradual birefringence loss at 500–30 min and all of the 600 MPa combination treatments. However, even at the highest pressure–lowest FC–longest HT (600–10%–30 min), random starch granules showing partial gelatinization (Figure 2; dashed

yellow arrow) and other swollen starch granules with a very hazy Maltese cross in the periphery were still observed. This is because higher pressure is more necessary for flour than its isolated starch counterpart to complete gelatinization due to the presence of non-starch components such as protein [41]. Overall, visually 500 MPa at 30 min HT, regardless of flour concentration, appeared to be a critical combination in the initiation of starch microstructure modification.

3.3. Three-Way ANOVA Results on Starch Properties and In Vitro Starch Digestibility as Affected by Pressure, Flour Concentration, and Holding Time

Tables 1 and 2 summarize significance values for the three-way and two-way interactions and the main effect of absorbance ratios, %RC, thermal properties, and starch digestion fractions. In general, a three-way interaction effect was detected for % RC, *To*, Δ*H*, and *DG*; no interaction was detected for Abs 1047/1022 and *Tc*, while the other parameters had at least one significant two-way interaction. This shows that the chosen variables have an evident influence on each other and are relevant HPP processing parameters.

Table 1. Summary of probability values after three-way ANOVA analysis of absorbance ratios, %RC, and starch digestion fractions as affected by pressure, flour concentration (FC), and holding time (HT).

Source of Variation	Abs 1047/1022	Abs 1022/995	%RC	%RDS	%SDS	%RS
Pressure	0.002	<0.001	<0.001	<0.001	<0.001	<0.001
FC	0.061	0.601	<0.001	0.011	0.010	<0.001
Time	0.053	0.307	0.014	0.062	0.010	0.005
Pressure ∗ FC	0.191	0.939	<0.001	0.147	0.020	0.151
Pressure ∗ HT	0.237	0.045	0.008	0.002	0.456	0.003
FC ∗ HT	0.139	0.450	0.929	0.368	0.601	0.351
Pressure ∗ FC ∗ HT	0.418	0.909	0.027	0.091	0.462	0.494

Table 2. Summary of probability values after three-way ANOVA analysis of thermal properties of cassava flour as affected by pressure, flour concentration (FC), and holding time (HT).

Source of Variation	*To*	*Tp*	*Tc*	*Trange*	Δ*H*	*DG*
Pressure	<0.001	<0.001	<0.001	0.039	<0.001	<0.001
FC	0.018	0.323	0.797	0.216	<0.001	<0.001
Time	<0.001	0.110	0.196	<0.001	<0.001	<0.001
Pressure ∗ FC	<0.001	0.015	0.590	0.194	<0.001	<0.001
Pressure ∗ HT	<0.001	0.024	0.960	<0.001	<0.001	<0.001
FC ∗ HT	0.104	0.874	0.466	0.111	0.502	0.377
Pressure ∗ FC ∗ HT	0.039	0.902	0.697	0.191	<0.001	<0.001

3.3.1. Short-Range Order of Cassava Starches

Short-range order is defined as the double-helical order and is related to variations in the ratio of the amounts of ordered to an unordered (amorphous) fraction within the starch granules [42]. The FTIR spectrum band at 1300–800 cm^{-1} is sensitive to starch granule's C–O–H bending [43]. Most previous works have identified bands at 1047, 1022, and 995 cm^{-1} to be sensitive to changes in the short-range order, representing the amount of ordered or crystalline starch, the amount of amorphous starch, and the influence of water content on the intramolecular hydrogen bonding, respectively [23]. The absorbance ratio of 1047/1022 cm^{-1} was used to quantify the ordered starch to amorphous starch [21], with a larger value being more crystalline [22], whereas 1022/995 cm^{-1} measures the molecular order of starch double helices, with an increased organization at a lower ratio [21,24].

No interactions were detected between the processing variables for 1047/1022 cm^{-1}, but a significant pressure effect was found (Table 1). Table 3 shows a notable decrease in the ratio, especially at 600–30 min. The FTIR spectra shown in Figure 3 for 875–1200 cm^{-1} also

displayed a decreased absorbance at pressure ≥500 MPa, similar to HPP-treated quinoa flour [11]. A notable decreasing band for 1047 cm^{-1} and an increasing 1022 cm^{-1} band were also observed, especially for 600–10% treatments. These imply a reduction in the short-range order and an increase in the amorphous starch fraction during gelatinization [23,42].

Table 3. Absorbance ratio values of untreated and HPP-treated cassava flours.

Pressure (MPa)	Flour Conc. (% *w*/*v*)	1047/1022		1022/995	
		10 min HT	30 min HT	10 min HT	30 min HT
0.10 (untreated)	10	0.65 ± 0.13		0.95 ± 0.03	
	20	0.87 ± 0.19		0.91 ± 0.25	
	30	0.80 ± 0.21		0.96 ± 0.04	
300	10	0.99 ± 0.09	0.79 ± 0.08	0.84 ± 0.16	0.94 ± 0.15
	20	0.83 ± 0.19	0.75 ± 0.13	1.00 ± 0.25	0.83 ± 0.09
	30	0.88 ± 0.06	0.84 ± 0.11	0.87 ± 0.13	0.83 ± 0.21
400	10	0.83 ± 0.11	0.70 ± 0.1	0.89 ± 0.12	1.07 ± 0.07
	20	0.79 ± 0.16	0.76 ± 0.13	0.98 ± 0.06	0.98 ± 0.18
	30	0.68 ± 0.11	0.84 ± 0.07	1.05 ± 0.03	1.01 ± 0.06
500	10	0.61 ± 0.05	0.73 ± 0.09	1.21 ± 0.24	1.27 ± 0.27
	20	0.85 ± 0.18	0.67 ± 0.11	1.16 ± 0.14	1.02 ± 0.13
	30	0.84 ± 0.10	0.87 ± 0.11	0.91 ± 0.05	1.20 ± 0.14
600	10	0.63 ± 0.09	0.54 ± 0.06	1.42 ± 0.32	1.09 ± 0.27
	20	0.86 ± 0.26	0.53 ± 0.05	1.34 ± 0.55	0.98 ± 0.21
	30	0.72 ± 0.15	0.66 ± 0.16	1.31 ± 0.44	1.02 ± 0.09

Results are presented as mean ± standard deviation of individual HPP treatment (n = 3).

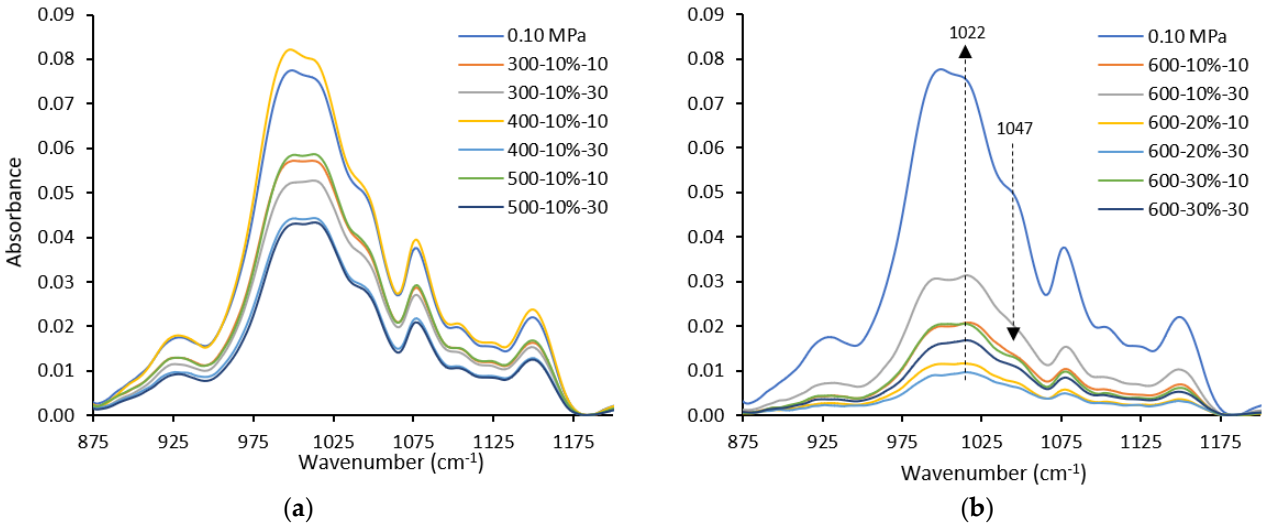

Figure 3. FTIR spectra of untreated (0.10 MPa) and selected HPP-treated flours at the 875–1200 cm^{-1} region; (**a**) 0.01 MPa and 300–500 MPa–10% flour concentration at both 10 and 30 mins; (**b**) 0.01 MPa and all 600 MPa combinations.

On the other hand, the absorbance ratio for 1022/995 cm^{-1} had a significant two-way interaction between pressure and time, with both having a significant simple main effect (Table 1). Warren, Gidley, and Flanagan [43] also found this ratio to be a valuable tool to monitor loss of structure, but a thorough assessment of spectra suggested greater complexity. Simple comparisons between pressures at 10 min HT ($p < 0.001$) revealed that 600 MPa was significantly higher compared to 0.1–400 MPa but not to 500 MPa, and was also not different from other pressures at 30 min HT. Hence, holding time was only significant at 600 MPa ($p = 0.002$), with 10 min having 0.328 units higher than 30 min

HT. Although the opposite was expected, this still shows that 600 MPa could reduce the molecular order of starch double helices.

3.3.2. Long-Range Order of Cassava Starches

The long-range order of starch granules can only be determined by XRD [43], which demonstrates the packing of double helices into ordered arrays [42]. From the diffractogram, the crystallinity from the long-range order was determined from the percentage of area under each prominent peak to the total area under the curve [25]. Analysis revealed a significant three-way interaction between pressure, FC, and HT (Table 1). The simple two-way interaction of pressure and FC against all levels of HT (both $p < 0.001$) and succeeding simple simple main effect of pressure across flour concentrations at certain levels of HT (all $p < 0.001$) were statistically significant at a significance level of 0.025%. Simple simple comparisons between pressures across all FCs at 10 min HT revealed that 600 MPa had significantly lowered %RC relative to other pressures, while no difference was found between lower pressures. This interaction is best visualized in Figure 4. On the other hand, at 10%–30 min, 500 MPa was significantly higher than 600 MPa but they were both significantly lower than other pressures. Conversely, at 20% to 30%–30 min, only 600 MPa was significantly lower than other pressures. The interaction between the variables demonstrated graduation in loss of %RC, which conforms with the varying degree of birefringence loss of the said samples. Furthermore, the statistically significant mean difference of 600 MPa to other pressures decreases with increasing FC at both HTs, revealing an inverse relationship of the hydration level of flour with %RC. However, the mean difference increased with HT between similar concentrations except for 10%, signifying a higher impact with longer HT. These suggest that 600 MPa is sufficient to alter the crystallinity or the long-range order of cassava starch in flour into a more amorphous state, but the intensity of alteration is dependent on flour concentration and holding time.

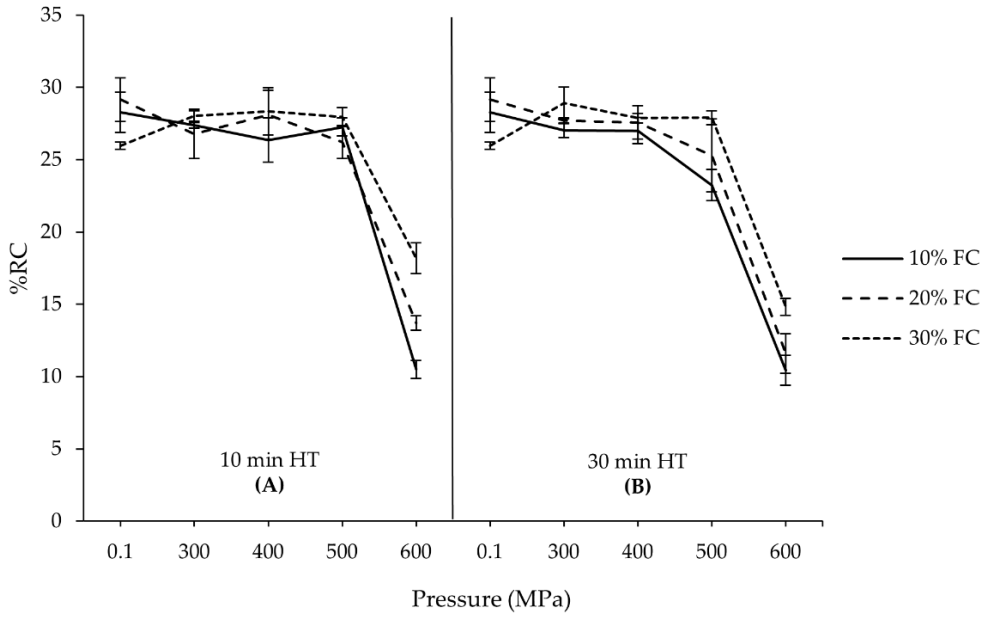

Figure 4. The relative crystallinity percentage (%RC) of untreated (0.1 MPa) and HPP-treated cassava flour at 10 min (**A**) and 30 min holding time (**B**). Error bars represent ± standard deviation (n = 3).

XRD graphs can also be utilized to compare changes in crystallinity visually. The cassava flour samples exhibited a type C polymorph with a stronger type A orientation. It was characterized by distinct single peaks at 2θ-15 and 23°, a double peak at 17.5°, and weak peaks at 20, 27, and 30°. No difference in spectra was observed from the control to all 400 MPa treatment combinations. However, at 500–10%–30, the intensity of the double

peak at 2θ-17.5° and single peaks at 15 and 23° was slightly reduced (Figure 5A), while it was maintained in other 500 MPa combinations. Figure 5B reveals that at 600 MPa, the peaks at 2θ-15 and 23° were dissolved progressively with decreasing FC and increasing HT. The doublet peak at 2θ-17.5° turned into a singlet with decreasing intensity as FC decreased and HT increased. A similar decrease in intensity was reported for buckwheat flour and ascribed to crystallinity loss during the HPP treatment [44]. Moreover, a more prominent 2θ-20° was observed, indicating the formation of amylose–lipid complexes during the process [17,44,45].

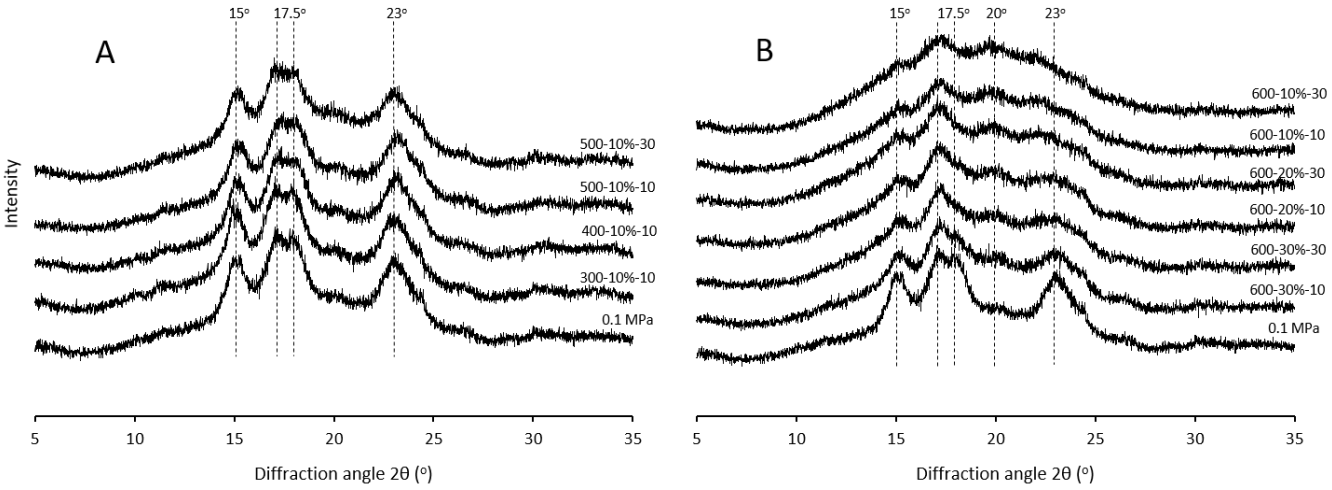

Figure 5. X-ray diffraction spectra of untreated (0.1 MPa) and selected HPP-treated cassava flours; where (**A**) shows spectra for untreated, 300 to 500–10%–10, and 500–10%–30, and (**B**) shows spectra for untreated and all 600 MPa treatment combinations.

3.3.3. Thermal Properties of HPP-treated Cassava Flours

The three-way ANOVA analysis of transitional gelatinization temperatures of cassava flours revealed that only *To* had a significant three-way interaction effect, and *Tp* had a two-way interaction effect (Table 2). Hence, *Trange* had a significant two-way interaction effect. However, no interaction was found for *Tc*. Further analysis on *To* revealed that there were significant simple simple main effects between pressures across all FC at 10 min HT (all $p < 0.001$) and at 20% and 30% FC for 30 min HT (both $p < 0.001$). Simple simple comparisons revealed that 600 MPa was consistently higher in *To* than other pressures in all FC and HT combinations (Figure 6A). Since no endothermic peak was detected at 600–10%–30, it was not included in the analysis. Nevertheless, this indicates full gelatinization of starch in the flour. The significant statistical mean difference between 600 MPa and other pressures decreased progressively with an increase in FC and prolonging HT. Other combinations of simple two-way interactions confirm this observation statistically. The significant two-way interaction of pressure with both FC and HT for *Tp* revealed a simple main effect result similar to *To*. This suggests that 600 MPa has an increasing effect on *Tp* regardless of the level of FC and HT, up until complete gelatinization. Despite the increase in both *To* and *Tp*, the interaction of pressure and HT on *Trange* revealed that the endothermic peak for gelatinization significantly narrowed by 0.93–1.56 °C at 600–30 min relative to other pressures and 1.96 °C narrower than 600–10 min. In the case of *Tc*, only a significant main effect was found, as seen in the similar sharp temperature increase at all 600 MPa treatment combinations. A rising shift in gelatinization temperatures was also observed in HPP-treated chestnut, oat, and quinoa flours [11,18,37], indicating the loss of the less stable crystalline structures [33].

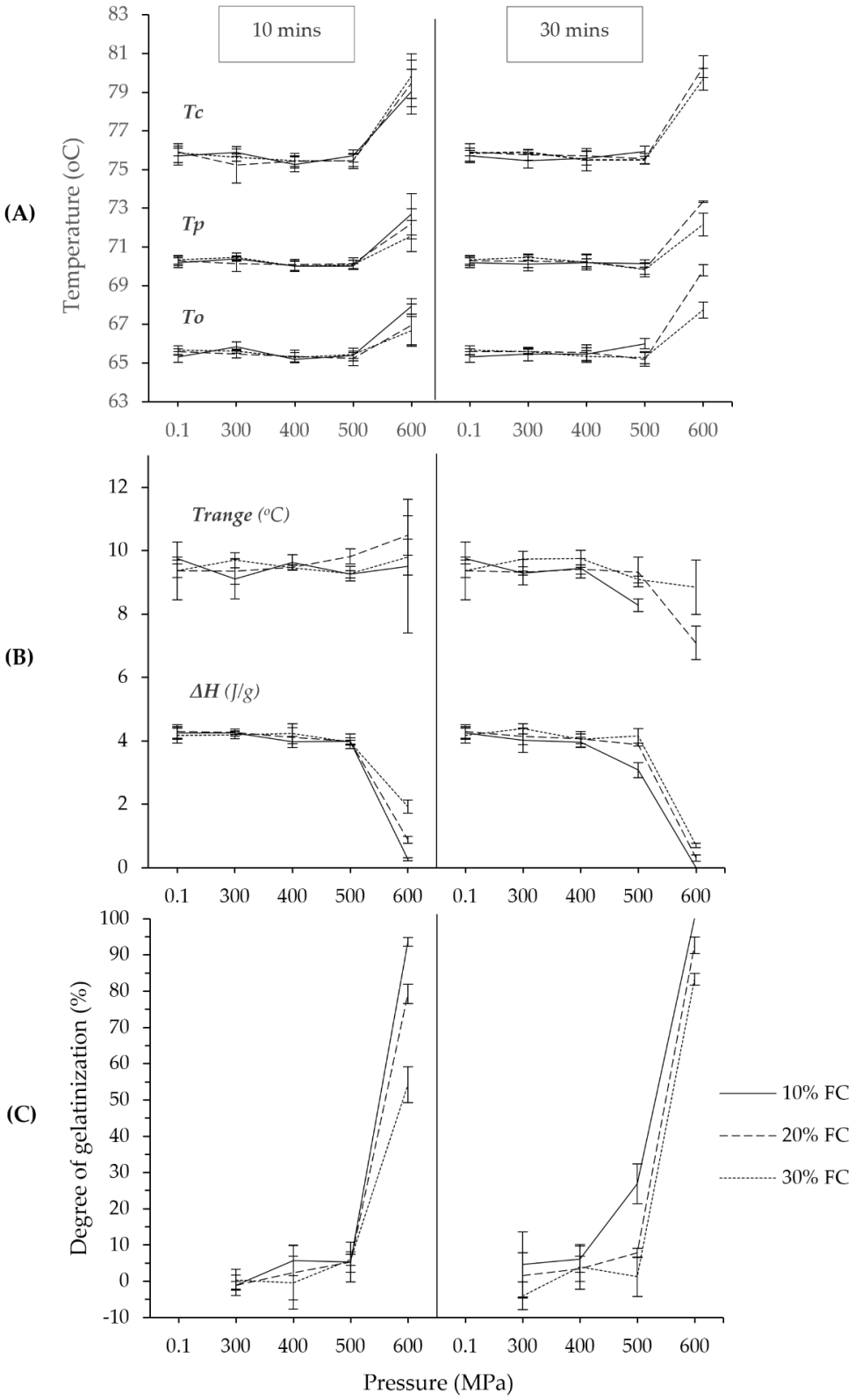

Figure 6. The thermal properties of untreated and HPP-treated cassava flour. (**A**) onset (*To*), peak (*Tp*), conclusion, and (*Tc*) gelatinization temperatures; (**B**) temperature range of gelatinization (*Trange*) and gelatinization enthalpy (Δ*H*); (**C**) degree of gelatinization. Error bars represent ± standard deviation (n = 3).

The change in gelatinization enthalpy (ΔH) and *DG* had significant three-way interactions and revealed similar results but inverse values. Both had significant simple two-way interactions between pressure and FC at different levels of HT (all $p < 0.001$) and a significant simple simple main effect between pressures on all levels of FC and HT (all $p < 0.001$). The ΔH was significantly lower at 600 MPa than other pressures regardless of FC at 10 min HT, while no difference was found between lower pressure combinations (Figure 6B). At 10%–30 min, 500 MPa was significantly higher than 600 MPa, but they were both significantly lower than other pressures. As no endothermic peak was detected at 600–10%–30, it was acknowledged to be fully gelatinized and recorded as 0 J/g or 100% *DG*. At 20% to 30%–30 min, only 600 MPa was significantly lower than other pressures. These results corroborate with %RC, as enthalpy change associated with gelatinization is measured by DSC and gelatinization involves the disruption of the ordered structure [43]. Consequently, a similar trend was seen in *DG* but with increasing values instead (Figure 6C).

3.3.4. Digestive Enzyme Susceptibility of Starches from HPP-Treated Cassava Flours

There was no three-way interaction found for %RDS, %SDS, and %RS; however, two-way interaction was found between pressure and either flour concentration (%SDS) or holding time (%RDS and %RS). Both %RDS and %RS had a significant simple main effect for pressure within each level of holding time (all $p < 0.001$) and a simple main effect of holding time at 500 MPa only ($p < 0.001$). Simple comparisons between pressures revealed that 600 MPa was significantly higher in %RDS than other pressures at 10 min HT by 3.42–3.76%, whereas at 30 min HT, both 500 and 600 MPa were significantly higher than other pressures but with 500 MPa significantly lower by 2.43% than 600 MPa. This means at higher HT, 500 MPa can already significantly increase the %RDS of cassava flour. An increase in digestibility has been reported in HPP-treated rice and waxy rice starches [46,47] and buckwheat flour [44], owing to microstructural damage in starch granules from gelatinization leading to easier access of enzyme to the inner structure. Despite this, starch digestibility of any HPP-treated starches was lower than their thermally treated counterpart [48,49]. The difference in starch granular integrity was postulated to be a factor. When starch is thermally gelatinized in excess water, it involves side-by-side dissociation of helices, followed by helix coil transitions and eventually a complete loss of granular structure [50]. Under pressure, the starch granule remains intact, as disintegration is incomplete since van der Waals and hydrogen bonds are stabilized, which favors the helix structure [8]. On the other hand, the simple comparisons between holding times showed that 500–30 min was 1.14% significantly higher in %RDS than 500–10 min, and yet, no HT dependency was observed for 600 MPa. This could mean that maximum hydrolysis can be achieved at 54% *DG* or 18% RC (600–30%–10), and no further pressure-induced gelation can increase its susceptibility to digestive enzymes. This is contrary to the results of Zeng et al. [46], wherein an increase in %RDS from 39 to ≈67% was observed for waxy rice starch with 0–58% *DG* or 0–29% RC. Potential reasons for this difference in values are the different in vitro starch digestibility protocols used and the starch substrate. The same trend of significant treatments was observed for %RS, albeit with receding values. The 600 MPa was significantly lower than other pressures at 10 min HT and 500 MPa at 30 min. The 500–30 min was significantly lower by 1.35% than 500–10 min and there was no difference between 600–10 min and 600–30 min. These interactions are illustrated in Figure 7A,B and evidently demonstrates increased susceptibility to digestive enzymes.

In the case of %SDS, a significant simple main effect between pressures within each level of flour concentration was found (10% $p = 0.021$, 20 and 30% $p < 0.001$). The %SDS in 0.1 MPa or untreated flour was not different from higher pressures at 10% FC but was significantly lower at 20% FC than 300–500 MPa, and only significantly lower than 500 MPa at 30% FC. Across the three flour concentrations, the %SDS in 500 MPa was significantly higher than 600 MPa. From the general trend and statistical data, it can be inferred that with an increase in pressure to 500 MPa, a significant decrease in %RS is coupled with an increase in %SDS and %RDS. A further reduction in %RS and an increase in %RDS can be

obtained at 600 MPa but with the reduction of %SDS (Figure 7C). Similarly, an increase in %SDS at 500 MPa and a decline when increased to 600 MPa was exhibited by waxy rice starch [46] and sweet potato flour [51]. SDS delivers a slow release of glucose in the blood; hence, HPP-treated cassava flours can be utilized as an ingredient in novel products exhibiting a lower glycaemic index.

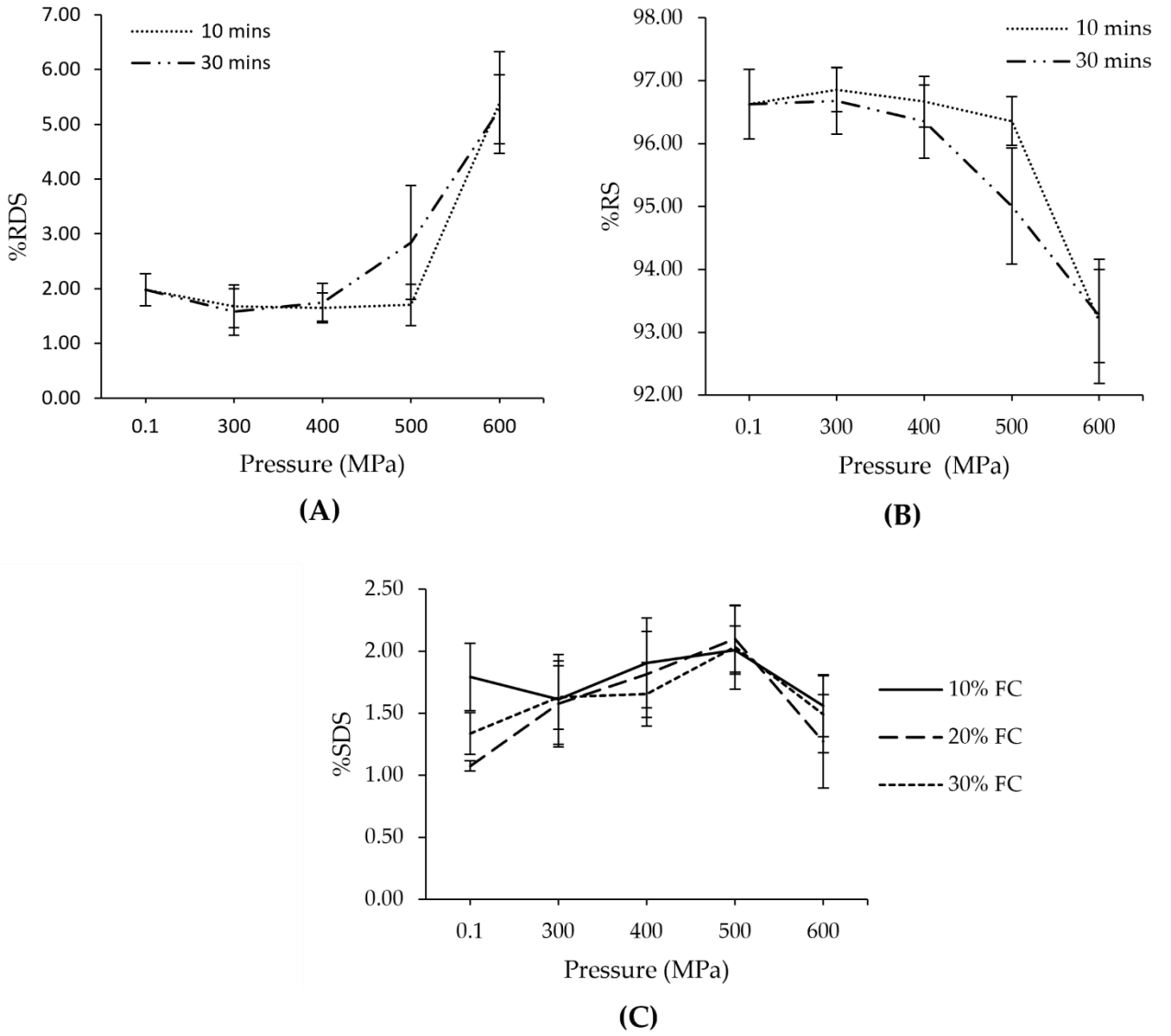

Figure 7. Two-way interactions of %RDS (pressure ∗ HT; (**A**)), %SDS (pressure ∗ FC; (**C**)), and %RS (pressure ∗ HT; (**B**)) for untreated and HPP-treated cassava flour. Rapidly digestible starch (RDS); slowly digestible starch (SDS); resistant starch (RS); and flour concentration (FC). Error bars represent ±standard deviation (n = 3).

4. Conclusions

The current work has provided increased insights into the impact of high hydrostatic pressure, flour concentration, and pressurizing holding time on cassava flour dispersions. Pressure-induced gelatinization of cassava starches in flour was initiated at 500 MPa, given high hydration and long holding time, and progressed at 600 MPa. The molecular disorder within the starch granules that comes with gelatinization led to the loss of birefringence, changes in FTIR starch bands, reduced crystallinity and gelatinization enthalpy, a rising shift in gelatinization temperatures, and increased susceptibility to digestive enzymes. The

significant interaction of processing variables resulted in a progressive impact on starch properties that increased with increasing pressure and holding time and decreasing flour concentration. In general, 600 MPa, regardless of flour concentration and holding time, significantly and consistently shifted the starch properties of cassava flour. Therefore, HPP can modify cassava flour through its inherent starch and create flours with varying levels of modification and functionalities, such as increasing the percentage of slowly digested starch, providing the possibility to produce novel products with a lower glycaemic index.

Author Contributions: Conceptualization, I.O., B.K. and L.A.C.; methodology, L.A.C., S.Y.L., B.K. and I.O.; formal analysis, L.A.C.; investigation, L.A.C., B.K. and I.O.; resources, I.O.; data curation, L.A.C.; writing—original draft preparation, L.A.C.; writing—review and editing, L.A.C., S.Y.L., B.K. and I.O.; visualization, L.A.C.; supervision, B.K. and I.O.; project administration, I.O.; funding acquisition, I.O. All authors have read and agreed to the published version of the manuscript.

Funding: This research was funded by the Manaaki New Zealand Scholarship through the Ministry of Foreign Affairs and Trade, and Riddet Institute, a New Zealand Centre of Research Excellence, funded by the Tertiary Education Commission.

Institutional Review Board Statement: Not applicable.

Informed Consent Statement: Not applicable.

Data Availability Statement: Not applicable.

Acknowledgments: L.A.C. would like to acknowledge the Manaaki New Zealand Scholarship through the Ministry of Foreign Affairs and Trade for her doctoral scholarship. Additionally, the authors would like to thank PhilRootcrops and Visayas State University, Baybay City, Leyte for the cassava roots provided and access to their facilities during flour production. I.O. and S.Y.L. are affiliated with the Riddet Institute, a New Zealand Centre of Research Excellence, funded by the Tertiary Education Commission.

Conflicts of Interest: The authors declare no conflict of interest. The funders had no role in the design of the study; in the collection, analyses, or interpretation of data; in the writing of the manuscript, or in the decision to publish the results.

References

1. Stapleton, G. Global starch market outlook and competing starch raw materials for by product segment and region. In Proceedings of the Cassava Starch World 2012, Phnom Penh, Cambodia, 22–24 February 2012.
2. Chisenga, S.M.; Workneh, T.S.; Bultosa, G.; Alimi, B.A. Progress in research and applications of cassava flour and starch: A review. *J. Food Sci. Technol.* **2019**, *56*, 2799–2813. [CrossRef] [PubMed]
3. Ocloo, F.C.K.; Ayernor, G.S. Production of alcohol from cassava flour hydrolysate. *J. Brew. Distill.* **2010**, *1*, 16–21. [CrossRef]
4. Aryee, F.N.A.; Oduro, I.; Ellis, W.O.; Afuakwa, J.J. The physicochemical properties of flour samples from the roots of 31 varieties of cassava. *Food Control* **2006**, *17*, 916–922. [CrossRef]
5. Ciacco, C.F.; D'Appolonia, B.L. Baking Studies with Cassava and Yam Flour. I. Biochemical Composition of Cassava and Yam Flour. *Cereal Chem.* **1978**, *55*, 402–411.
6. Kim, H.-S.; Kim, B.-Y.; Baik, M.-Y. Application of Ultra High Pressure (UHP) in Starch Chemistry. *Crit. Rev. Food Sci. Nutr.* **2012**, *52*, 123–141. [CrossRef]
7. Pei-Ling, L.; Xiao-Song, H.; Qun, S. Effect of high hydrostatic pressure on starches: A review. *Starch Stärke* **2010**, *62*, 615–628. [CrossRef]
8. Knorr, D.; Heinz, V.; Buckow, R. High pressure application for food biopolymers. *(BBA) Proteins Proteom.* **2006**, *1764*, 619–631. [CrossRef]
9. Yang, Z.; Chaib, S.; Gu, Q.; Hemar, Y. Impact of pressure on physicochemical properties of starch dispersions. *Food Hydrocoll.* **2017**, *68*, 164–177. [CrossRef]
10. Ahmed, J.; Mulla, M.Z.; Arfat, Y.A.; Kumar, V. Effects of High-Pressure Treatment on Functional, Rheological, Thermal and Structural Properties of Thai Jasmine Rice Flour Dispersion. *J. Food Process. Preserv.* **2017**, *41*, e12964. [CrossRef]
11. Zhu, F.; Li, H. Effect of high hydrostatic pressure on physicochemical properties of quinoa flour. *LWT* **2019**, *114*, 108367. [CrossRef]
12. Lin, T.; Fernández-Fraguas, C. Effect of thermal and high-pressure processing on the thermo-rheological and functional properties of common bean (*Phaseolus vulgaris* L.) flours. *LWT* **2020**, *127*, 109325. [CrossRef]
13. McCann, T.H.; Leder, A.; Buckow, R.; Day, L. Modification of structure and mixing properties of wheat flour through high-pressure processing. *Food Res. Int.* **2013**, *53*, 352–361. [CrossRef]

14. Lee, N.-Y.; Koo, J.-G. Effects of high hydrostatic pressure on quality changes of blends with low-protein wheat and oat flour and derivative foods. *Food Chem.* **2019**, *271*, 685–690. [CrossRef] [PubMed]
15. Hüttner, E.K.; Dal Bello, F.; Arendt, E.K. Fundamental study on the effect of hydrostatic pressure treatment on the bread-making performance of oat flour. *Eur. Food Res. Technol.* **2010**, *230*, 827–835. [CrossRef]
16. Ahmed, J.; Mulla, M.Z.; Arfat, Y.A. Particle size, rheological and structural properties of whole wheat flour doughs as treated by high pressure. *Int. J. Food Prop.* **2017**, *20*, 1829–1842. [CrossRef]
17. Ueno, S.; Sasao, S.; Liu, H.; Hayashi, M.; Shigematsu, T.; Kaneko, Y.; Araki, T. Effects of high hydrostatic pressure on β-glucan content, swelling power, starch damage, and pasting properties of high-β-glucan barley flour. *High Press. Res.* **2019**, *39*, 509–524. [CrossRef]
18. Ahmed, J.; Al-Attar, H. Structural properties of high-pressure-treated chestnut flour dispersions. *Int. J. Food Prop.* **2017**, *20*, S766–S778. [CrossRef]
19. Perez, S.; Bertoft, E. The molecular structures of starch components and their contribution to the architecture of starch granules: A comprehensive review. *Starch Stärke* **2010**, *62*, 389–420. [CrossRef]
20. Liu, G.; Li, J.; Shi, K.; Wang, S.; Chen, J.; Liu, Y.; Huang, Q. Composition, Secondary Structure, and Self-Assembly of Oat Protein Isolate. *J. Agric. Food Chem.* **2009**, *57*, 4552–4558. [CrossRef]
21. Xiao, J.; Niu, L.; Wu, L.; Li, D.; He, H. Preparation of an In Vitro Low-Digestible Rice Starch by Addition of Grass Carp Protein Hydrolysates and Its Possible Mechanisms. *Starch Stärke* **2019**, *71*, 1800159. [CrossRef]
22. Xia, W.; Wang, F.; Li, J.; Wei, X.; Fu, T.; Cui, L.; Li, T.; Liu, Y. Effect of high speed jet on the physical properties of tapioca starch. *Food Hydrocoll.* **2015**, *49*, 35–41. [CrossRef]
23. Van Soest, J.J.G.; Tournois, H.; De Wit, D.; Vliegenthart, J.F.G. Short-range structure in (partially) crystalline potato starch determined with attenuated total reflectance Fourier-transform IR spectroscopy. *Carbohydr. Res.* **1995**, *279*, 201–214. [CrossRef]
24. Guo, Z.; Zhao, B.; Chen, L.; Zheng, B. Physicochemical Properties and Digestion of Lotus Seed Starch under High-Pressure Homogenization. *Nutrients* **2019**, *11*, 371. [CrossRef]
25. Rafiq, S.I.; Jan, K.; Singh, S.; Saxena, D.C. Physicochemical, pasting, rheological, thermal and morphological properties of horse chestnut starch. *J. Food Sci. Technol.* **2015**, *52*, 5651–5660. [CrossRef] [PubMed]
26. Krueger, B.R.; Knutson, C.A.; Inglett, G.E.; Walker, C.E. A Differential Scanning Calorimetry Study on the Effect of Annealing on Gelatinization Behavior of Corn Starch. *J. Food Sci.* **1987**, *52*, 715–718. [CrossRef]
27. Minekus, M.; Alminger, M.; Alvito, P.; Ballance, S.; Bohn, T.; Bourlieu, C.; Carrière, F.; Boutrou, R.; Corredig, M.; Dupont, D.; et al. A standardised static in vitro digestion method suitable for food—An international consensus. *Food Funct.* **2014**, *5*, 1113–1124. [CrossRef]
28. Abduh, S.B.M.; Leong, S.Y.; Agyei, D.; Oey, I. Understanding the Properties of Starch in Potatoes (Solanum tuberosum var. Agria) after Being Treated with Pulsed Electric Field Processing. *Foods* **2019**, *8*, 159. [CrossRef]
29. Englyst, H.N.; Kingman, S.M.; Cummings, J.H. Classification and measurement of nutritionally important starch fractions. *Eur. J. Clin. Nutr.* **1992**, *46*, S33–S50.
30. Breuninger, W.F.; Piyachomkwan, K.; Sriroth, K. Chapter 12—Tapioca/Cassava Starch: Production and Use. In *Starch*, 3rd ed.; BeMiller, J., Whistler, R., Eds.; Academic Press: San Diego, CA, USA, 2009; pp. 541–568.
31. Asaoka, M.; Blanshard, J.M.V.; Rickard, J.E. Seasonal Effects on the Physico-chemical Properties of Starch from Four Cultivars of Cassava. *Starch Stärke* **1991**, *43*, 455–459. [CrossRef]
32. Pei-Ling, L.; Qing, Z.; Qun, S.; Xiao-Song, H.; Ji-Hong, W. Effect of high hydrostatic pressure on modified noncrystalline granular starch of starches with different granular type and amylase content. *LWT* **2012**, *47*, 450–458. [CrossRef]
33. Katopo, H.; Song, Y.; Jane, J.-l. Effect and mechanism of ultrahigh hydrostatic pressure on the structure and properties of starches. *Carbohydr. Polym.* **2002**, *47*, 233–244. [CrossRef]
34. Larrea-Wachtendorff, D.; Sousa, I.; Ferrari, G. Starch-Based Hydrogels Produced by High-Pressure Processing (HPP): Effect of the Starch Source and Processing Time. *Food Eng. Rev.* **2021**, *13*, 622–633. [CrossRef]
35. Vittadini, E.; Carini, E.; Chiavaro, E.; Rovere, P.; Barbanti, D. High pressure-induced tapioca starch gels: Physico-chemical characterization and stability. *Eur. Food Res. Technol.* **2008**, *226*, 889–896. [CrossRef]
36. Cappa, C.; Lucisano, M.; Barbosa-Cánovas, G.V.; Mariotti, M. Physical and structural changes induced by high pressure on corn starch, rice flour and waxy rice flour. *Food Res. Int.* **2016**, *85*, 95–103. [CrossRef]
37. Hüttner, E.K.; Dal Bello, F.; Poutanen, K.; Arendt, E.K. Fundamental evaluation of the impact of high Hydrostatic Pressure on oat batters. *J. Cereal Sci.* **2009**, *49*, 363–370. [CrossRef]
38. Biliaderis, C.G. Chapter 8—Structural Transitions and Related Physical Properties of Starch. In *Starch*, 3rd ed.; BeMiller, J., Whistler, R., Eds.; Academic Press: San Diego, CA, USA, 2009; pp. 293–372.
39. Błaszczak, W.; Valverde, S.; Fornal, J. Effect of high pressure on the structure of potato starch. *Carbohydr. Polym.* **2005**, *59*, 377–383. [CrossRef]
40. Song, M.-R.; Choi, S.-H.; Kim, H.-S.; Kim, B.-Y.; Baik, M.-Y. Efficiency of high hydrostatic pressure in preparing amorphous granular starches. *Starch Stärke* **2015**, *67*, 790–801. [CrossRef]
41. Ahmed, J.; Ramaswamy, H.S.; Ayad, A.; Alli, I.; Alvarez, P. Effect of high-pressure treatment on rheological, thermal and structural changes in Basmati rice flour slurry. *J. Cereal Sci.* **2007**, *46*, 148–156. [CrossRef]

42. Sevenou, O.; Hill, S.E.; Farhat, I.A.; Mitchell, J.R. Organisation of the external region of the starch granule as determined by infrared spectroscopy. *Int. J. Biol. Macromol.* **2002**, *31*, 79–85. [CrossRef]
43. Warren, F.J.; Gidley, M.J.; Flanagan, B.M. Infrared spectroscopy as a tool to characterise starch ordered structure—A joint FTIR–ATR, NMR, XRD and DSC study. *Carbohydr. Polym.* **2016**, *139*, 35–42. [CrossRef] [PubMed]
44. Zhou, Z.; Ren, X.; Wang, F.; Li, J.; Si, X.; Cao, R.; Yang, R.; Strappe, P.; Blanchard, C. High pressure processing manipulated buckwheat antioxidant activity, anti-adipogenic properties and starch digestibility. *J. Cereal Sci.* **2015**, *66*, 31–36. [CrossRef]
45. Lopez-Rubio, A.; Flanagan, B.M.; Gilbert, E.P.; Gidley, M.J. A novel approach for calculating starch crystallinity and its correlation with double helix content: A combined XRD and NMR study. *Biopolymers* **2008**, *89*, 761–768. [CrossRef]
46. Zeng, F.; Li, T.; Gao, Q.; Liu, B.; Yu, S. Physicochemical properties and in vitro digestibility of high hydrostatic pressure treated waxy rice starch. *Int. J. Biol. Macromol.* **2018**, *120*, 1030–1038. [CrossRef]
47. Deng, Y.; Jin, Y.; Luo, Y.; Zhong, Y.; Yue, J.; Song, X.; Zhao, Y. Impact of continuous or cycle high hydrostatic pressure on the ultrastructure and digestibility of rice starch granules. *J. Cereal Sci.* **2014**, *60*, 302–310. [CrossRef]
48. Stute, R.; Heilbronn; Klingler, R.W.; Boguslawski, S.; Eshtiaghi, M.N.; Knorr, D. Effects of High Pressures Treatment on Starches. *Starch Stärke* **1996**, *48*, 399–408. [CrossRef]
49. Papathanasiou, M.M.; Reineke, K.; Gogou, E.; Taoukis, P.S.; Knorr, D. Impact of high pressure treatment on the available glucose content of various starch types: A case study on wheat, tapioca, potato, corn, waxy corn and resistant starch (RS3). *Innov. Food Sci. Emerg. Technol.* **2015**, *30*, 24–30. [CrossRef]
50. Waigh, T.A.; Gidley, M.J.; Komanshek, B.U.; Donald, A.M. The phase transformations in starch during gelatinisation: A liquid crystalline approach. *Carbohydr. Res.* **2000**, *328*, 165–176. [CrossRef]
51. Cui, R.; Zhu, F. Physicochemical properties and bioactive compounds of different varieties of sweetpotato flour treated with high hydrostatic pressure. *Food Chem.* **2019**, *299*, 125129. [CrossRef] [PubMed]